Articles

Theoretical Studies of the Early Stage Coagulation Kinetics for a Charged Colloidal Dispersion

K. L. Wu and S. K. Lai*

Complex Liquids Laboratory, Department of Physics, National Central University, Chung-li 320, Taiwan

Received September 19, 2004. In Final Form: January 21, 2005

We study the early stage coagulation kinetics for a charged colloidal dispersion which is here modeled by an effective two-body colloid−colloid potential. The colloidal system was physically prepared by choosing sets of colloidal parameters varying in particular the Hamaker constant and the particle's size. The kinetics of coagulation process was driven by the addition of an indifferent electrolyte and assumed to proceed in two quasi-steady steps. In the first step, colloidal particles are destabilized by the presence of a second potential minimum to diffuse from a bulk-stabilized liquid phase to a flocculated phase. In the second step, we assume that different entities are found in the second potential minimum. The entities comprise secondary dimers, secondary dimers undergoing redispersion, and monomers still in singlet states. If, under favorable condition, this kind of interaction-driven diffusive motion continues, a fraction of the secondary dimers will be induced to undergo primary dimers formation in the first deep minimum. Whether or not the latter process occurs is determined either energetically by the potential barrier falling below a prescribed value, say of $15k_BT$, or/and the second potential minimum becoming negligibly small (with a magnitude $<k_BT$). A prototype example to exhibit this kind of the coagulation kinetics phenomenon is an aqueous dispersion of polystyrene latex particles. Our detailed analysis on this system showed the connection between the change of rate constants and the reversible flocculation⇄irreversible coagulation transition and would throw a fresh light on the use of both the energy and the kinetic criteria for understanding the colloidal stability such as those observed in the liquid−liquid coexistence.

Introduction

The study of the aggregation and stability of charged colloidal dispersions has had a long history. Interest in this specific property can be traced to its industrial applications and to its increasing importance in environmental problems. Academically, the issue of the mechanisms of colloidal stability, though existing for nearly a century, remains a great challenge to the soft condensed matter theorists. The difficulties in understanding the stability of colloids lie in the complexity between colloids and small ions (counterions plus co-ions) their Coulomb interactions which are intrinsically many-body in nature. The tendency for a colloidal dispersion to remain either in a charge-stabilized disperse state or in a state showing aggregation depends on a number of factors. These include the particle size, particle charge (or surface potential), colloidal and electrolyte concentrations, and material property of the particles and the environment in which they disperse (Hamaker constant). Stability of charged colloids can be studied in two general approaches. The first approach is based on the energy criterion where one places emphasis on the thermal collisions of colloidal particles and investigates the possibility of the thermally collided particles being trapped into the first deep potential minimum resulting in an irreversible coagulation. It is intuitively felt that in order to prevent the energetic particles from falling into the first deep potential minimum, a high barrier maximum has to be maintained. The second approach is based on the kinetic criterion. Here, one studies the time evolution behavior of the diffusion-driven colloidal particles. In the present case, the temporal process depends on the details of interactions between colloids and small ions. If the thermodynamic condition is such that a second potential well (believed to be the mechanism giving rise to the reversible flocculation) exists, and particles are happened to be trapped there, the kinetic effect of charged colloids can be understood from the time of coagulation.

The simplest aggregation kinetics for the charged colloidal system is to study the early stage formation of dimers when the dispersion is induced by some externally controlled parameters, such as the temperature or an electrolyte.[1−3] Theoretically the pioneering work of Smoluchowski[4] has laid a general foundation in the study of coagulation kinetics. Smoluchowski developed a theory to calculate the rate of rapid coagulation based on the assumption that colloidal particles, under high electrolyte concentration, are driven to approach each other. At each encounter, the colloidal particles are assumed to have the possibility of adhesion and hence permitting one to identify the rate of coagulation as the frequency of encounters. His theory of rapid coagulation was somewhat simplified

* To whom correspondence should be addressed. E-mail: sklai@coll.phy.ncu.edu.tw.

(1) Velegol, D.; Anderson, J. L.; Garoff, S. *Langmuir* **1996**, *12*, 675. Velegol, D.; Anderson, J. L.; Garoff, S. *Langmuir* **1996**, *12,* 4103.
(2) Buil, S.; Delville, J. P.; Freysz, E.; Ducasse, A. *Opt. Lett*. **1998**, *23*, 1334.
(3) Buil, S.; Delville, J. P.; Ducasse, A. *Phys. Rev. Lett.* **1999**, *82*, 1895.
(4) Smoluchowski, von M. *Phys. Z.* **1916**, *17*, 557; *Z. Phys. Chem.* **1917**, *92*, 129.

10.1021/la0476682 CCC: $30.25
Published on Web 03/11/2005

and has subsequently been quantified to reflect more realistic situations. Fuchs[5,6] stressed the role of repulsive interaction, introduced the stability ratio W, being the diffusion fluxes for rapid and slow coagulations, and studied the change of W due to the mutual diffusion of colloidal particles. Brenner,[7] Spielman,[8] and Honig et al.[9] later included the hydrodynamic interaction into the theory of Fuchs. A related work on the kinetics of the early stage of aggregation by Ruckenstein[10] should perhaps be mentioned. Ruchenstein followed mainly the idea of Fuchs and, in two consecutive steps, assumed quasi-steady-state diffusions created by the force field between two particles. The first step concerns the quasi-steady-state diffusion for particles in the bulk fluid and for those being trapped in the second potential minimum, and the second step aims at the quasi-steady-state diffusion in the force field between the second and first potential minima. Since the first and second potential minima were treated equally and assumed in his work to be of comparable order of magnitudes, the relative importance of the aggregation of particles in both minima was analyzed. Complication of the calculations has limited his studies of the aggregation kinetics to employing linearized rate equations. An improvement to the work of Ruckenstein in which one determines the stability ratio by combined treatment of the primary minimum coagulation and the secondary minimum flocculation was proposed in the following year by Marmur.[11] Marmur computed W by relaxing the steady-state assumption. His theoretical calculation interpreted satisfactorily the experimental data concerning the particle size dependence of W. The results Marmur reported clearly point to the importance of the second potential minimum in accounting for the colloidal stability. It is therefore not surprising to see some of the earlier theoretical and experimental studies on colloidal systems[12−17] already devoted to examining the role played by the second minimum in colloid−colloid potential. More recently, the issue of the second potential minimum has been revisited experimentally by Hachisu[18] for the case of two coexisting phases in gold sol, and theoretically by Kaldasch et al.,[19] Lai et al.,[20,21] and Morales et al.[22] for studies of the liquid−liquid coexisting phases, as well as by Behrens and Borkovec[23] for the early stage aggregation kinetics problems. In our theoretical calculations, we have applied a thermodynamic perturbation theory to calculate the phase diagrams of charged colloids and used the energy criterion to understand the reversible flocculation⇄irreversible coagulation scenario. Still, there remain ambiguities in the calculated phase diagrams (Figure 4 in Lai and Wu[21]) since the energy barrier for the predicted stable liquid-liquid coexisting phases is unrealistically low. The colloidal stability for this system needs thus to be examined kinetically. Turning to the coagulation kinetics, earlier works[10,11,24,25] focused more on calculating W in a qualitative manner. More recent efforts,[23,26−28] on the other hand, have directed attention to compute the rate constants which account semiquantitatively for the kinetic consequence. Among them the recent communication of Behrens and Borkovec[23] is one such endeavor which is of direct relevance to the present work.

Motivation for the present work is twofold. First, we shall examine the energy criterion often used in analyzing the colloidal stability results deduced from phase diagrams. We shall compare the findings between the energetic stability and those predicted kinetically. The colloidal dispersions would be energetically and kinetically self-consistent if both criteria reach the same conclusion. Second, there are now available experiments on the early stage kinetics of phase-separated liquid mixtures.[2,3] The use of a semiquantitative approach[23] in conjunction with a realistic colloid−colloid potential of mean force to evaluate the rate constants for dimers aggregation will be an invaluable first step toward a more completed theory of aggregation. The layout of the paper is as follows. In the following section, we review briefly the colloid−colloid potential to be used in the present work to describe the force-field-induced diffusion. Then, we give the rate equations for dimers and derive formulas for the rate constants in terms of the colloid−colloid potential. Hydrodynamic interaction to account for the viscous diffusive process will be included. Next, we present numerical results for the early stage kinetics of charged colloids with input data drawn from experiments. An implication deduced from the calculated rate constants is discussed. The same analysis is further applied to concrete examples taken from our previous phase diagram results. In conclusion, we summarize the main findings in this work and comment on the possible drawback and limitation related to our present theoretical studies.

Theory of Kinetic of Coagulation

Two-Body Colloid−Colloid Interaction Potential. To find the interaction energy of any two colloidal particles in a colloidal dispersion, we consider an aqueous colloidal system consisting of charged colloids each with size σ_0 and charge Z_0 and a collection of counterions and other added electrolytes whose sizes and charges are (σ_1, Z_1)

(5) Fuchs, N. *Z. Phys.* **1934**, *89,* 736.
(6) Verwey, E. J.; Overbeek, J. G. *Theory of the Stability of Lyophobic Colloids*; Elsevier: Amsterdam, 1948.
(7) Brenner, H. *J. Colloid Interface Sci.* **1965**, *20*, 104. Brenner, H. *J. Colloid Interface Sci.* **1967**, *23*, 407.
(8) Spielman, L. A. *J. Colloid* I*nterface Sci.* **1970**, *33*, 562.
(9) Honig, E. P.; Roebersen, G. J.; Wiersema, P. H. *J. Colloid Interface Sci.* **1971**, *36*, 97.
(10) Ruckenstein, E. J. *J. Colloid Interface Sci*. **1978**, *66*, 531.
(11) Marmur, A. *J. Colloid Interface Sci.* **1979**, *72*, 41.
(12) Schenkel, J. H.; Kitchener, J. A. *Trans. Faraday Soc.* **1960**, *56*, 161.
(13) Wiese, G. R.; Healy, T. W. *Trans. Faraday Soc.* **1970**, *66*, 490.
(14) Watillon, A.; Joseph-Petit A. M. *Discuss. Faraday Soc*. **1966**, *42*, 143.
(15) Ottewill, R. H.; Shaw, J. N. *Discuss. Faraday Soc*. **1966**, *42*, 154.
(16) Long, J. A.; Osmond, D. W. J.; Vincent, B. *J. Colloid Interface Sci.* **1973**, *42*, 545.
(17) Victor, J. M.; Hansen, J. P. *J. Chem. Soc., Faraday Trans.* **1985**, *81*, 43.
(18) Hachisu, S. *Croat. Chem. Acta* **1998**, *71*, 975.
(19) Kaldasch, J.; Laven, J.; Syein, H. N. *Langmuir* **1996**, *12*, 6197.
(20) Lai, S. K.; Peng, W. P.; Wang, G. F. *Phys. Rev.* **2001**, *63*, 041511-1.
(21) Lai, S. K.; Wu, K. L. *Phys. Rev. E* **2002**, *66*, 041403-1.
(22) Morales, V.; Anta, J. A.; Lago, S. *Langmuir* **2003**, *19*, 475. It is relevant to comment that this paper applied the reference hypernetted chain integral equation to study the stability of charged colloidal suspensions. The authors compared their calculated phase diagram κ vs η with our previous work (ref 20) and with the Monte Carlo simulation and concluded that our calculated results show somewhat larger discrepancies. We should remark that the perturbation theory used in ref 20 is in first order and the pair correlation function employed there is the Percus−Yevick hard-sphere closure, both of which are indeed approximate. An extension of the perturbation theory to second order and including a more accurate Verlet−Weis (Verlet, L.; Weis, J. J. *Phys. Rev. A* **1972**, *5*, 939) pair correlation function has subsequently been developed (ref 21). The calculated κ vs η agrees better with the Monte Carlo simulation.
(23) Behrens, S. H.; Borkovec, M. *J. Colloid Interface Sci.* **2000**, *225*, 460.
(24) Lifson, S.; Jackson, J. L. *J. Chem. Phys*. **1962**, *36*, 2410.
(25) Sauer, S.; Löwen, H. *J. Phys.*: *Condens. Matter* **1996**, *8*, L803.
(26) Simonin, J. P.; Hendrawan, H. *Phys. Chem. Chem. Phys.* **2001**, *3*, 4286.
(27) Odriozola, G.; Leone, R.; Schmitt, A.; Callejas-Fernandez, J.; Martinez-Garcia, R.; Hidalgo-Alvarez, R. *J. Chem. Phys.* **2004**, *121*, 5468. See also references therein.
(28) Ivanov, K. L.; Lukzen, N. N. *J. Chem. Phys.* **2004**, *121*, 5109.

and ($\sigma_i, Z_i, i = 2, 3, ...$), respectively. The system is therefore intrinsically multicomponents and the corresponding Ornstein−Zernick (OZ) equations read

$$h_{ij}(r) = c_{ij}(r) + \sum_{\ell=0} \rho_\ell \int h_{i\ell}(|\mathbf{r} - \mathbf{r}'|)\, c_{\ell j}(r')\, \mathrm{d}\mathbf{r}' \quad (1)$$

The indices $i, j,$ and ℓ refer to different species: $i, j, \ell = 0$ for colloids, $i, j, \ell = 1$ for counterions, and $i, j, \ell = 2, 3, ...$ for co-ions. Here, ρ_ℓ is the number density for species ℓ; $c_{ij}(r)$ is the direct correlation function, and $h_{ij}(r) = g_{ij}(r) - 1$ is the total correlation function defined in terms of the pair correlation function $g_{ij}(r)$. A realistic model for describing the system is the primitive model where one considers the particles as a mixture of charged hard spheres characterized by different diameters and charges. It has been shown in the literature[29,30] that for pointlike small ions (counterions plus co-ions) and via some kind of mathematical manipulation, eq 1 can be reduced to an effective one-component OZ equation. Within the mean spherical approximation, the resulting OZ equation can be solved analytically for the effective direct correlation function as

$$c_{00}^{\mathrm{eff}}(r) = -(Z_0 X)^2 L_\mathrm{B} \frac{\mathrm{e}^{-k_\mathrm{D} r}}{r}, \quad r > \sigma_0 \quad (2)$$

where $k_\mathrm{D}^2 = \sum_{i=1} \alpha_i^2$ (we define generally $\alpha_i^2 = 4\pi L_\mathrm{B} \rho_i Z_i^2$ the Bjerrum length $L_\mathrm{B} = e^2\beta/(4\pi\epsilon\epsilon_0)$ where $\beta = 1/(k_\mathrm{B}T)$ is the inverse temperature). In terms of the reduced small ions concentration $\kappa = k_\mathrm{D}\sigma_0$, $X = \cosh(\kappa/2) + U[(\kappa/2)\cosh(\kappa/2) - \sinh(\kappa/2)]$ in which $U = 8\delta/\kappa^3 - 2\nu/\kappa$ with $\delta = 3\eta_0/(1 - \eta)$, where $\eta_0 = \pi\sigma_0^3\rho_0/6$, $\nu = [(\Gamma\sigma_0/2 + \delta)/(1 + \Gamma\sigma_0/2 + \delta]$ and

$$\Gamma^2 = k_\mathrm{D}^2 + \frac{\alpha_0^2}{(1 + \Gamma\sigma_0/2 + \delta)^2} \quad (3)$$

which has to be solved iteratively for Γ given Z_0, σ_0, κ, and η, and hence X in eq 2. It is interesting to note that X tends to $\exp(\kappa/2)/(1 + \kappa/2)$ for $\rho_0 \to 0$ which is the Derjaguin−Landau−Verwey−Overbeek (DLVO)[6] limit. Since these equations are all solved within the mean spherical approximation closure, it is natural to identify the right-hand side of eq 2 as the two-body colloid−colloid potential of mean force, i.e.

$$\beta\phi(x) = (Z_0 X)^2 L_\mathrm{B} \mathrm{e}^{-\kappa} \frac{\mathrm{e}^{-\kappa(x-1)}}{x}, \quad x > 1 \quad (4)$$

where $x = r/\sigma_0$ is the reduced distance, and for the convenience of discussion below, we define $T_\Lambda = (Z_0 X)^2 L_\mathrm{B} \mathrm{e}^{-\kappa}/k_\mathrm{B}$. We shall employ $\phi(x)$ to describe the repulsive interaction potential for the charged colloids. To study the stability of colloids, we supplement to eq 4 the (nonretarded) van der Waals attraction $v_{\mathrm{vdw}}(r)$ given by

$$v_{\mathrm{vdw}}(r) = -\frac{AH(x)}{12} \quad (5)$$

where A is the Hamaker constant and

$$H(x) = 1/(x^2 - 1) + 1/x^2 + 2\ln(1 - 1/x^2) \quad (6)$$

The total potential energy function is thus given by

$$u(r) = \phi(r) + v_{\mathrm{vdw}}(r) \quad (7)$$

Equation 7 constitutes a useful expression for our recent calculations of phase diagrams and is further used in this work to study the kinetics of the coagulation problem.

Rate Equations for Dimer. Following Sonntag and Strenge[31] and Behrens and Borkovec,[23] let us consider a system of monodisperse colloids at a given number density ρ_0. In the disperse state each colloid can be treated as a monomer which we denote here by M. When the principal barrier height is low and the second minimum is negligible, we expect to observe the rapid aggregation of primary dimers in a one-step reaction process given by

$$2\mathrm{M} \xrightarrow{k} \mathrm{P} \quad (8)$$

where k is the rate constant containing information for two monomers M aggregated to form a primary dimer. If, on the other hand, we have a reasonably high potential barrier (say on the order $15k_\mathrm{B}T$ or higher) and a sufficiently deep second minimum (a few $k_\mathrm{B}T$ say) whose well depth and position are given by $u(r_\mathrm{m})$ and r_m (schematically shown in Figure 1 below) respectively, the aggregation process of dimers needs to be modified into two steps. First, $u(r_\mathrm{m})$ will hold the monomers to form secondary dimers S. However, in view of the weaker strength of $u(r_\mathrm{m})$, dimers S have the likelihood of either redispersing reversibly into monomers M again or, when the barrier height is indeed low, proceeding to the first minimum and aggregating irreversibly to become primary dimers P. This two-step reaction is mathematically expressed by

$$2\mathrm{M} \underset{k_2}{\overset{k_1}{\rightleftharpoons}} \mathrm{S} \xrightarrow{k_3} \mathrm{P} \quad (9)$$

Since $u(r_\mathrm{m})$ is generally less deep, it is possible for the reversible flocculation to occur and this is accounted for by the rate constant k_2. Denoting $n_1(t)$, $n_{2\mathrm{S}}(t)$, and $n_{2\mathrm{P}}(t)$ as the number concentrations of monomers, secondary dimers, and primary dimers, respectively, at time t, these quantities satisfy the following rate equations

$$\frac{\mathrm{d}n_1(t)}{\mathrm{d}t} = -k_1 n_1^2(t) + 2k_2 n_{2\mathrm{S}}(t) \quad (10)$$

$$\frac{\mathrm{d}n_{2\mathrm{S}}(t)}{\mathrm{d}t} = \frac{1}{2} k_1 n_1^2(t) - (k_2 + k_3) n_{2\mathrm{S}}(t) \quad (11)$$

$$\frac{\mathrm{d}n_{2\mathrm{P}}(t)}{\mathrm{d}t} = k_3 n_{2\mathrm{S}}(t) \quad (12)$$

Implicit in this set of coupled equations is the assumption of a very deep first minimum.[32] Note also that the formation of primary dimers depends on the concentration of secondary dimers if higher order aggregates such as trimers, tetramers, etc. can be neglected (early stage approximation). This condition is justified if concentrations

(29) Lai, S. K.; Wang, G. F. *Phys. Rev. E* **1998**, *58*, 3072.
(30) Belloni, L. *J. Chem. Phys.* **1986**, *85*, 519.
(31) Sonntag, H.; Strenge, K. *Coagulation Kinetics and Structure Formation*; Plenum: New York, 1987.
(32) Prieve, D. C.; Ruckenstein, E. *J. Colloid Interface Sci.* **1980**, *73*, 539.

of dimers formed are much less than those of the monomers. Thus, given k_i, eqs 10−12 can be solved numerically for the time evolution of $n_1(t)$, $n_{2S}(t)$, and $n_{2P}(t)$. We now turn to consider the rate constants k_i.

Formulas for Rate Constants. In the absence of a potential second minimum, k in eq 8 is given by[31,33]

$$k^{-1} = \int_{\sigma_0}^{\infty} \frac{\exp[\beta u(r)]}{4\pi r^2 D(r)}\, dr \tag{13}$$

which describes the early stage process of an irreversible aggregation of monomers to form primary dimers. In writing eq 13, it is assumed that the particles forming primary dimers can mutually approach each other up to the contact distance σ_0. The $D(r)$ in eq 13 is the relative pair diffusion coefficient introduced to incorporate the viscous interaction between particles and to account for the deviation of the assumption of additivity of single particle Brownian diffusivities during coagulation. For a spherically symmetric relative motion, $D(r)$ appears in the modified Smoluchoski equation[31] given by

$$\frac{\partial n_i(r,t)}{\partial t} = -\mathrm{div} J_{ij} \tag{14}$$

in which $J_{ij} = J_{ij}^{D} + J_{ij}^{u}$ where $J_{ij}^{D} = -(1/\beta f_{ij}) = -D_{ij}(r)(\partial n_i(r,t)/\partial r)$ (Fick's law relation) and $J_{ij}^{u} = -(n_i(r,t)/f_{ij})(\partial u(r)/\partial r)$ are respectively the relative diffusion flux density and the relative flux density resulting from the action of $u(r)$ and $n_i(r,t)$ is the number density distribution of the centers of particles i in the proximity of particles j. The f_{ij} is the hydrodynamic resistance coefficient for relative motion and is shown in the literature[8,34,35] to depend on the viscosity, particle dimensions, and the relative separation r between Brownian particles at centers i and j. Accordingly, the relative pair diffusion coefficient D_{ij} has a r-dependence attributable to f_{ij}. Now, when the physical condition is such that there exists a second potential minimum in $u(r)$, the mutually approaching particles will likely first form secondary minimum dimers at r_m and then, if condition permits, will proceed to the first potential minimum to form primary dimers, otherwise they will undergo a redispersion. Since $u(r_m)$ is generally of the order of a few k_BT much weaker than the first minimum, we need to consider the latter possibility of a reversible flocculation. In other words, eq 13 has to be modified to account first for the secondary dimer formation. Assuming a quasi steady state for the secondary aggregation, we obtain from eq 13 the number density distribution

$$\frac{n_i}{n_i^{\infty}} = \frac{\exp(-\beta u(r)) \int_{r_m}^{r} \frac{\exp(\beta u(r'))}{r'^2 D_{ij}(r')}\, dr'}{\int_{r_m}^{\infty} \frac{\exp(\beta u(r'))}{r'^2 D_{ij}(r')}\, dr'} \tag{15}$$

in three consecutive steps: first setting $\partial n_i(r,t)/\partial t = 0$, then performing an integration once, and finally applying the boundary conditions: at $r = r_m$ for $n_i = 0$, $u(r) \to u(r_m)$ and at $r = \infty$ for $n_i = n_i^{\infty}$, $u(r) \to 0$. Substituting eq 15 into J_{ij}^{D} and J_{ij}^{u} the constant $k_1^{-1} = -(4\pi r^2 J_{ij}/n_i^{\infty})$ can be shown[31] to read

$$k_1^{-1} = \int_{r_m}^{\infty} \frac{\exp[\beta u(r)]}{4\pi r^2 D(r)}\, dr \tag{16}$$

where the subscript ij in $D(r)$ is dropped hereafter. Given k_1, the reversible rate constant k_2 can be determined by the principle of detailed balance, viz.

$$k_1/k_2 = 2VQ_2/Q_1^2 \tag{17}$$

where V is the total volume of the system and Q_j is the j-particle canonical partition function ($j = 1$ for monomer and $j = 2$ for dimer). Substituting the two-particle partition function Q_2 and the single-particle Q_1 into eq 17, we arrive at

$$k_2^{-1} = k_1^{-1} \int_{r_M}^{r_{out}} r^2 \exp[-\beta u(r)]\, dr \tag{18}$$

where r_M is the position of the potential barrier maximum, r_{out} is the outer maximum of the integrand of eq 16 which is defined to be the limit such that two particles lying between r_M and r_{out} will be considered as forming a (secondary) dimer and

$$k_3^{-1} = (k_1/k_2) \int_{\sigma_0}^{r_m} \frac{\exp[\beta u(r)]}{r^2 D(r)}\, dr \tag{19}$$

These are three rate constants explicitly expressed in terms of $u(r)$ and $D(r)$. It remains to find $D(r)$. In this work, we use the $D(r)$ formula given by Honig et al.[9] Denoting D_S to be the single-particle diffusion coefficient, the additivity assumption of single particle Brownian diffusivities amounts to assigning $2D_S$ to the relative pair diffusion coefficient. The resulting $D(r)$ is

$$D(r) = 2D_S/B(2y/\sigma_0) \tag{20}$$

where $y = r - \sigma_0$ is the separation distance, and

$$B(y) = (6y^2 + 13y + 2)/(6y^2 + 4y) \tag{21}$$

is a hydrodynamic correction factor.[9,31]

Parenthetically, we should remark that the same rate constants k_2^{-1} and k_3^{-1} can be obtained alternatively from the Smoluchowski-type diffusion equation[36−38]

$$\frac{\partial P(r,t)}{\partial t} = \frac{1}{r^2} \frac{\partial}{\partial r}\left[r^2 D(r) \left(\frac{\partial P(r,t)}{\partial r} + \beta P(r,t) \frac{\partial u(r)}{\partial r} \right) \right] \tag{22}$$

Here the function $P(r,t)$ is the probability for a pair of particles separated by a distance r at time t. In actual application of eq 22 to derive k_i^{-1}, $P(r,t)$ may *not* be needed explicitly. Instead one makes use of eq 22 to obtain a reaction time $\Lambda_i = k_i^{-1}$ which is the average time required for a particle, beginning at some point and moving under the influence of $u(r)$ to arrive at and be bound to a target particle. Szabo et al.[36] and Deutch[37] have separately derived a general formula for Λ_i (see eqs 2.15 and 6 in refs 36 and 37, respectively) in this so-called first passage time approach.[38] Starting with the formula Λ_i, it is possible to obtain the rate constants if appropriate boundary condi-

(33) Russel, W. B.; Saville, D. A.; Schowalter, W. R. *Colloidal Dispersions*; Cambridge University Press: Cambridge, 1989.
(34) Maude, A. D. *Br. J. Appl. Phys.* **1961**, *12*, 293.
(35) Stimson, M.; Jeffery, G. B. *Proc. R. Soc. London* **1926**, *111*, 110.
(36) Szabo, A.; Schulten, K.; Schulten, Z. *J. Chem. Phys.* **1980**, *72*, 4350.
(37) Deutch, J. M. *J. Chem. Phys.* **1980**, *73*, 4700.
(38) Hänggi, P.; Talkner, P.; Borkovec, M. *Rev. Mod. Phys.* **1990**, *62*, 251.

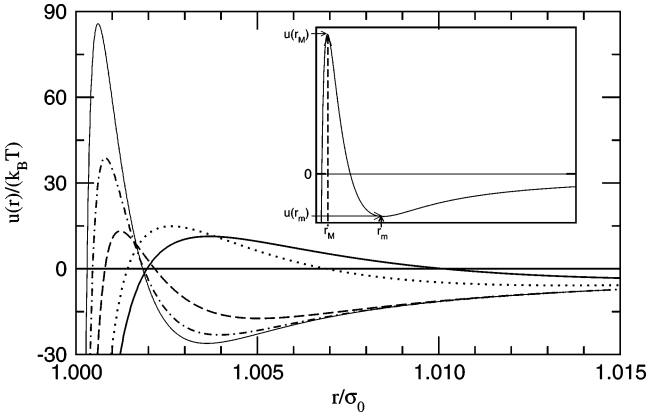

Figure 1. Plot of two-body colloid−colloid potential $u(r)$ vs reduced distance r/σ_0 for five aqueous latex dispersions calculated with the colloidal parameters given in Table 1 (taken from Kotera et al.[39]) within the DLVO approximation. Notation for the curves is as follows: full, $\sigma_0 = 350$ nm; dotted, $\sigma_0 = 416$ nm; dashed, $\sigma_0 = 758$ nm; dash−dotted, $\sigma_0 = 1078$ nm; thin full, $\sigma_0 = 1374$ nm.

tions are imposed. We finally note in passing that a conceptually similar approach to derive the rate constants has previously been proposed by Lifson and Jackson.[24]

Discussion

Experimental Results: Reversible Flocculation vs Irreversible Coagulation. It is instructive to first analyze the experimental results of Kotera et al.[39] who studied the role of $u(r_m)$ on the transition between the reversible flocculation and the irreversible coagulation for a series of "soap-free" polystyrene latex particles using the optical method as well as the electron microscopy. Figure 1 displays the colloid−colloid potentials calculated within the DLVO approximation ($\rho_0 \rightarrow 0$ in eqs 4 and 7 above) with input data σ_0, κ, and ψ_0 taken directly from their measurements. The Hamaker constant is set to be $A = 1.3 \times 10^{-20}$ J, which is a value estimated by the authors to be reasonable. Let us scrutinize these $u(r)$ from the viewpoint of energy criterion. One notices first of all two broad kinds of $u(r)$. The first kind, to which systems $\sigma_0 =$ 350 and 416 nm belong, is characterized by $u(r)$ attaining a somewhat lower first maximum barrier $u(r_M)$ at $r = r_M$ (see Figure 1) and a relatively shallower $u(r_m)$ which is located quite far out. These colloidal suspensions therefore do not a priori possess the $u(r_m)$ and $u(r_M)$ of sufficient strength or magnitude as to breed for the formation of secondary dimers. Since the prepared latex dispersions are at their critical flocculation concentrations, any further addition of electrolytes to them will have the effect of inducing an irreversible coagulation if the thermally collided particles have sufficient energy to circumvent $u(r_M)$. Indeed, Kotera et al. observed the scenarios of irreversible coagulations in their light transmission coefficient experiments for these two latex dispersions. Coming to the second kind, to which the remaining three colloidal dispersions belong, the physical conditions are such that $u(r)$ shows a clear deep $u(r_m)$ in addition to exhibiting a significant barrier height ($u(r_M) > 15k_BT$). Now, the presence of a deep $|u(r_m)|$ ($> 15k_BT$) accompanied by a sufficiently high $u(r_M)$ generally enhances the formation of secondary dimers and hence the subsequent aggregating tendency for trimers, tetramers, etc. In fact, Kotera et al. have repeated several times their light transmission coefficient measurements for the present three systems and compared them with the two colloidal dispersions of the first kind. Their results demonstrated clearly that this second kind of latex particle is fully redispersable. This agglomeration phenomenon, based mainly on the energy criterion, has been employed in the literature[17,20−22] to discuss the stability of charged colloids. A question arises: Are these colloidal dispersions kinetically stable?

To delve into this issue, we now turn to study the early stage process of the kinetics of coagulation. Table 1 summarizes the results of k_1, k_2, and k_3 and other related quantities for the same aqueous latex dispersions calculated using eqs 16, 18, and 19 with the same set of colloidal parameters as in Figure 1. Two features deserve emphasis. First, the transient time[40] $\tau = 1/(k_2 + k_3)$ is intimately related to $u(r_m)$ and $u(r_M)$ and its magnitude increases many orders of magnitudes in approaching the reversible flocculation from the irreversible coagulation. In Kotera et al.'s experiments, the former occurs for $\sigma_0 >$700 nm while the latter for $\sigma_0 <$400 nm; the threshold transition lies somewhere between $\sigma_0 \approx$ 400−700 nm. Generally, the rate constants satisfy $k_2 \gg k_3$ for $\sigma_0 >$400 nm. Second, the rate constants k_2 and k_3 both decrease with increasing σ_0, and quantitatively, the decrease in k_3 is more dramatic in contrast to k_2. The first feature points to a rapid growth of $u(r_M)$ and the concurrent development of a deep $u(r_m)$ with increasing σ_0. As a consequence, it considerably reduces the possibility of redispersed particles to come closer or any secondary dimer to proceed further to the first potential minimum that would favor the formation of primary dimers. The second feature implies that one can anticipate observing an increase in the number of secondary dimers in the second minimum for a longer period of time when large magnitudes of both $u(r_m)$ and $u(r_M)$ are simultaneously seen to show up. In Kotera et al.'s experiments, colloidal particles of size $\sigma_0 \geq$700 nm are seen to aggregate reversibly, possibly in the form of secondary dimers at the early stage kinetic process of coagulation. We depict in Figures 2 and 3 contributions of $n_{2S}(t)$, $n_{2P}(t)$, and $n_2(t)$ separately for the five different latex systems given in Table 1. Let us begin with Figure 2a for the system $\sigma_0 = 350$ nm. There is predicted a rapidly linear growth of an insignificantly small fraction of the secondary dimers for a duration $t \ll 0.106$ s (linearly extrapolated value from the amplified figure given in the same row next to Figure 2a). This is nonnegligible compared to the primary dimers $n_{2P}(t)$ whose value is virtually vanishing for the same duration. As $t \gg 0.106$ s, $n_{2P}(t)$ increases rapidly, and for $t \gtrsim 255$ s, it dominates over $n_{2S}(t)$. The aggregation time $t \approx 255$ s, where $n_{2P} = n_{2S}$ may thus be taken to mark the incipience of an irreversible aggregation since after which time we expect the dimers to proceed all the way to aggregate irreversibly. The latex particles with size $\sigma_0 = 416$ nm probably mark the very beginning of a change in kinetics of the coagulation process. This is evident by observing that for although $u(r_m)$ is slightly deeper, its magnitude is still rather shallow. For this latex dispersion, the potential barrier is, however, higher reaching $u(r_M) > 15k_BT$, which is a value customarily taken to be the amount of thermal energy just about for collided particles to satisfy the energy

(39) Kotera, A.; Furusawa, K.; Kubo, K. *Kolloid Z. Z. Polym.* **1970**, *240*, 837.

(40) The transient time τ is here introduced as a time scale for the convenience of discussion below. If the decrease in the concentration of monomers is negligible, viz., $n_1(t) \approx n_0$, n_0 being the initial concentration of monomers, it can be shown that eqs 10−12 yield (see ref 23) $n_{2S}(t) = (n_0^2/2)(k_1/(k_2 + k_3))[1 - e^{-(k_2+k_3)t}]$ and $n_{2P}(t) = (n_0^2/2)$-$(k_1k_3/(k_2+k_3))[t + (1/(k_2+k_3))(e^{-(k_2+k_3)t} - 1)]$. The aggregation time may be compared roughly with $\tau = 1/(k_2 + k_3)$ to deduce the linear time behaviors of $n_{2i}(t)$.

Table 1. Latex Particle Size σ_0 (nm), Reduced Electrolyte Concentration $\kappa = k_D\sigma_0$, Surface Potential ψ_0 (mV), Barrier Height $u(r_M)$ (k_BT), Position of Barrier Height r_M (nm), Depth of Second Minimum $u(r_m)$ (k_BT), Position of Second Minimum r_m (nm), Rate Constants k_1, k_2, and k_3 (Calculated by eqs 16, 18, and 19, respectively), and Transient Time $\tau = (k_2 + k_3)^{-1}$ for the Total Potential Energy Functions of Five Latices[a]

latices	σ_0	κ	ψ_0	$u(r_M)$	r_M	$u(r_m)$	r_m	k_1 (m^3 s^{-1})	k_2 (s^{-1})	k_3 (s^{-1})	τ (s)
SL-1	350	213	23	11.33	351.29	−3.79	356.81	7.66×10^{-18}	14.48	0.0291	0.069
SL-105	416	302	25	14.89	417.09	−5.83	421.67	7.66×10^{-18}	2.35	1.61×10^{-5}	0.42
SL-107	758	746	27	13.17	758.92	−17.4	761.82	7.66×10^{-18}	1.98×10^{-5}	1.07×10^{-9}	5.06×10^{4}
SL-114	1078	1010	28	38.82	1078.87	−23.1	1082.26	7.66×10^{-18}	3.42×10^{-8}	1.73×10^{-23}	2.92×10^{7}
SL-104	1374	1182	29	85.74	1374.84	−26.1	1378.96	7.66×10^{-18}	1.02×10^{-9}	2.61×10^{-45}	9.97×10^{8}

[a] Calculations for all colloidal systems were carried out using the same Hamaker temperature $T_A = A/k_B = 942$ K and were kept near room temperature, 293 K.

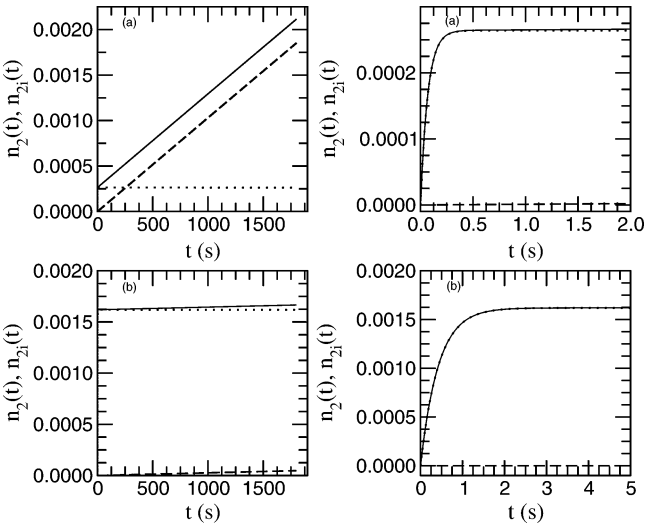

Figure 2. (a) Secondary $n_{2S}(t)$ (dotted curve), primary $n_{2P}(t)$ (dashed curve), and total $n_2(t) = n_{2S}(t) + n_{2P}(t)$ (full curve) concentrations of dimers vs time t (s) calculated for $\sigma_0 = 350$ nm within the DLVO approximation with rate constants k_1, k_2, and k_3 taken from Table 1. The plot on the right-hand side of the same row depicts $n_{2i}(t)$ and $n_2(t)$ for a very short time. (b) Same legend as in Figure 2a, but for $\sigma_0 = 416$ nm.

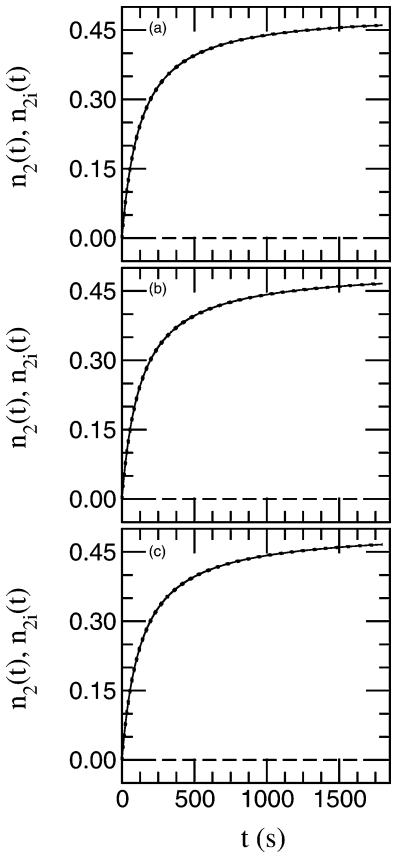

Figure 3. (a) Same legend as in Figure 2a, but for $\sigma_0 = 758$ nm. (b) Same legend as in Figure 2a, but for $\sigma_0 = 1078$ nm. (c) Same legend as in Figure 2a, but for $\sigma_0 = 1374$ nm.

criterion.[17,20,21] There is thus an increase in $n_{2S}(t)$ and it lasts for a longer period ($t \approx 0.474$ s) in comparison to that of $\sigma_0 = 350$ nm ($t \approx 0.106$ s). The fact that $n_{2S}(t)$ ($n_{2P}(t)$) mildly decreases (increases) at long time indicates that this colloidal dispersion, kinetically, is still weakly stable. Nevertheless, τ (=0.42 s) for this system is already an order of magnitude larger than that of the system $\sigma_0 =$ 350 nm ($\tau = 0.069$ s), and its $n_{2S}(t)$ is seen to increase an order of magnitude larger as well. It is interesting to note further that τ for the three remaining latex dispersions $\sigma_0 = 758$, 1078, and 1374 nm are many orders of magnitudes larger resulting in their corresponding $n_{2S}(t)$, shown in parts a−c of Figure 3 respectively, increases steadily, and by contrast, their respective $n_{2P}(t)$ almost vanishes with practically no formation of primary dimers.

Theoretical Results: Reversible Flocculation vs Irreversible Coagulation. It is of interest to ask if the experimental results discussed above suggest the same kinetic trend for our theoretical phase-diagram studies[21] on charged colloids. In our recent study on such a problem,[20,21] we established for the calculated phase diagram T vs η the threshold transition differentiating a reversible flocculation from an irreversible coagulation. The main idea in this energy criterion is as follows. Suppose a low-density liquid coexists with a high-density liquid. Thermodynamically, there should exist a critical temperature T_c above which the suspension is a homogeneous liquid and below which the liquid−liquid phase separation occurs. Since the two-body colloid−colloid potential is characterized by a potential barrier $u(r_M)$, and at high salt concentrations, a second potential minimum $u(r_m)$ as well, we proposed, somewhat judiciously, that the condition for the threshold transition satisfies $u(r_M) = 15k_BT_0$, T_0 being an undetermined temperature. This energy criterion manifests the amount of energy just sufficient to prevent the thermally collided colloidal particles to fall into the first deep minimum. Now, if T_0 is set equal to T_c whose value was imposed to satisfy $T_c \geq 273$ K (freezing point of water solvent), we sought for solutions in terms of the coupling constant T_Λ (defined just below eq 4), T_A, and κ subject to the energy constraint $u(r_M) = 15k_BT_c$. In this way, we obtained the phase diagram T_Λ vs T_A at given T_c. Note that along the $T_\Lambda - T_A$ curve κ is a maximum ionic concentration, κ_{max} say, which should be determined self-consistently in the Belloni model for various possible sets of (T_Λ, T_A) (see Lai et al.[20,21] for technical details). The $T_\Lambda - T_A$ phase boundary therefore demarcates the region of reversible flocculation (for $\kappa < \kappa_{max}$) from that of the irreversible coagulation (for $\kappa > \kappa_{max}$). We give in Figure 4a the (energy) stability curve for $T_c = 293$ K. For concreteness, we select three colloidal dispersions: the threshold ($\sigma_0^{min} = 340.3$ nm, $T_\Lambda^{min} =$

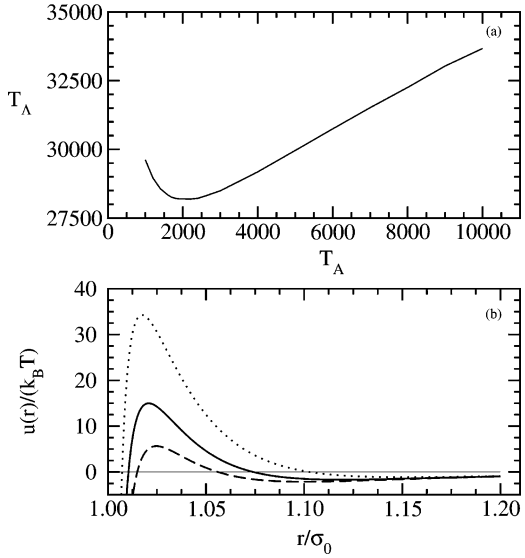

Figure 4. (a) Stability curve T_Λ vs T_A for a charged colloidal dispersion at critical temperature $T_c = 293$ K (see text). Along this curve, the maximum reduced electrolyte concentration is $\kappa = 38.37$. The dispersion will show reversible liquid−liquid stable phases for $\kappa < \kappa_{max}$ and irreversible coagulation for $\kappa > \kappa_{max}$. (b) Two-body colloid−colloid potential of mean force $u(r)$ vs r/σ_0 for $\kappa = 35 < \kappa_{max}$ (dotted curve), $\kappa_{max} = 38.37$ (full curve), and $\kappa = 40 > \kappa_{max}$ (dashed curve).

Table 2. Coupling Strength T_Λ, Size σ_0 (nm), Reduced Electrolyte Concentration $\kappa = k_D\sigma_0$, Rate Constants k_1, k_2, and k_3 (Calculated by eqs 16, 18, and 19, respectively), and Transient Time $\tau = (k_2 + k_3)^{-1}$ [a]

T_Λ	σ_0	κ	k_1 (m^3 s^{-1})	k_2 (s^{-1})	k_3 (s^{-1})	τ (s)
40000	457.5	35	1.02×10^{-17}	12.75	2.38×10^{-13}	0.0784
30745	340.3	38.37	1.01×10^{-17}	20.98	7.68×10^{-5}	0.0476
25000	271.3	40	1.01×10^{-17}	30.83	1.05	0.031

[a] The colloidal dispersion has the volume fraction $\eta_0 = 0.18$ and is calculated at critical temperature $T_c = 293$ K with the Hamaker temperature $T_A = 6000$ K.

30745, $\kappa_{max} = 38.37$), above threshold ($\sigma_0 = 457.5$ nm, $T_\Lambda = 40000$, $\kappa = 35$), and below threshold ($\sigma_0 = 271.3$ nm, $T_\Lambda = 25000$, $\kappa = 40$). All of these three dispersions are kept at the fixed $T_A = 6000$ K. Consistent with the energy criterion, the suspension above (below) threshold exhibits a reversible flocculation (irreversible coagulation). This is evident from reading Figure 4b that $u(r_M)$ above (below) threshold attains a higher (lower) value and a stable liquid−liquid transition is possible (less likely). The inchoate stage of coagulation kinetics is compatible also with the energy criterion if we analyze the calculated k_i detailed in Table 2. The trend of the change as well as the magnitudes of k_2 and k_3 are both in line with results deduced from Kotera et al.'s experiments, although the magnitudes of the transient time τ given in Table 2 are many orders of magnitudes smaller. To illustrate further, we display in Figure 5 the $n_{2S}(t)$ and $n_{2P}(t)$ vs t for these three colloidal dispersions. In going from above the threshold ($\kappa = 35$), via threshold ($\kappa_{max} = 38.37$), to below the threshold ($\kappa = 40$), we see subtle changes in $n_{2S}(t)$ and $n_{2P}(t)$ vs t. For $\kappa = 35$, $n_{2S}(t)$ increases linearly after an initial rapid growth for $t \leq 0.08$ s; for $\kappa_{max} = 38.37$, $n_{2S}(t)$ behaves similarly but increases more rapidly over a shorter period; and finally, for $\kappa = 40$, $n_{2S}(t)$ switches over to a rapid growth of $n_{2P}(t)$ at $t \approx 0.9$ s after a much shorter period of increase of $n_{2S}(t)$. It thus appears that for the kind of stability curve given in Lai and Wu[21] the energy and kinetic criteria work consistently.

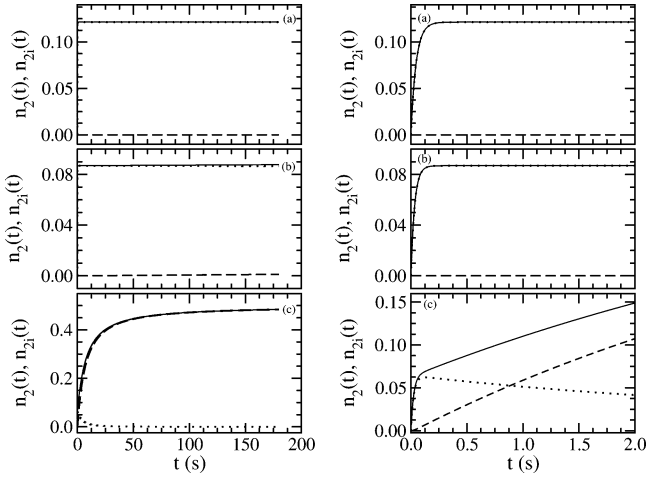

Figure 5. Secondary $n_{2S}(t)$ (dotted curve), primary $n_{2P}(t)$ (dashed curve), and total $n_2(t) = n_{2S}(t) + n_{2P}(t)$ (full curve) concentrations of dimers vs time t (s) calculated for (a) $\kappa = 35$, (b) $\kappa_{max} = 38.37$, and (c) $\kappa = 40$ with rate constants k_1, k_2, and k_3 taken from Table 2. The plot on the right-hand side of each row depicts $n_{2i}(t)$ and $n_2(t)$ for a very short time.

Theoretical Results: Phase Diagram of κ vs η. We turn next to an investigation of the early stage coagulation kinetics for the charged colloidal suspension whose stability criterion is described previously by the energy factor. Table 3 summarizes as in Table 1 related colloidal parameters along with the rate constants k_i. Before analyzing these results, we digress for a moment and make a few relevant remarks. First, the phase-diagram calculations in Lai and Wu[21] were done by appealing to the Weeks−Chandler−Andersen (WCA)[41] thermodynamic perturbation theory. Within WCA, $u(r)$ in eq 7 was used to construct the Helmholtz free energy and the usual thermodynamic conditions of imposing equal pressure and chemical potential were then applied to determine the phase diagrams. Second, the phase-diagram calculations given in Lai and Wu[21] were carried out at sufficiently high salt concentrations (>mM); the contribution of volume terms to the free energy function can therefore be ignored.[42,43] Third, as pointed out above, we have prepared our charged colloidal dispersions by monitoring either the size σ_0 at fixed A (simulating the attractive strength, see eq 5) which, for convenience, has been written as "temperature" $T_A = A/k_B$ or the T_A at fixed σ_0. Fourth, the stable or metastable liquid−liquid coexisting phases for all of the colloidal dispersions given in this table were calculated with respect to their respective liquid−solid counterparts. Finally, we have employed the approximate formula $Z_0 = \pi\psi_0\epsilon_0\sigma_0(2 + \kappa)$ where the surface potential is confined to values $\psi_0 \leq 25$ mV to ensure the reasonableness of eq 4. Let us now return to Table 3. Except in one case in $T_A = 4650$ K, k_3 in all of the colloidal dispersions considered are generally much smaller in magnitude than their corresponding k_2 implying thus that the formation of primary dimers should be less dominant. We note further two interesting aspects. The first aspect is that for systems with fixed T_A the stable liquid−liquid coexisting phases are described by smaller σ_0, being 700 nm at $T_A = 5800$ K and 200 nm at $T_A = 4650$ K. The trends of the changes of k_2 and k_3 in each group of dispersions are,

(41) Weeks, J. D.; Chandler, D.; Andersen, H. C. *J. Chem. Phys.* **1971**, *54*, 5237.
(42) Van Roij, R.; Hansen, J. P. *Phys. Rev. Lett.* **1997**, *79*, 3082.
(43) Wang, G. F.; Lai, S. K. *Phys. Rev. E* **2004**, *70*, 051402-1; see also the commentary (ref 20) of Lai, S. K.; Peng, W. P.; Wang, G. F. *Phys. Rev. E* **2001**, *63*, 041511-1.

Table 3. Hamaker $T_A = A/k_B$, Colloidal Size σ_0 (nm), Colloidal Volume Fraction η_0, Reduced Small Ions Concentration $\kappa = k_D\sigma_0$, Barrier Height $u(r_M)$ (k_BT), Position of Barrier Height r_M (nm), Depth of Second Minimum $u(r_m)$ (k_BT), Position of Second Minimum r_m (nm), Position of Outer Maximum r_{out} (nm) (See Text), Rate Constants k_1, k_2, and k_3 (Calculated by eqs 16, 18, and 19, respectively), and Transient Time $\tau = (k_2 + k_3)^{-1}$ for the Total Potential Energy Functions Correspond to the Critical Point Below Which the Stable or Metastable Liquid−Liquid Phases Coexist with Respect to the Liquid−Solid Counterparts[a]

T_A	σ_0	η_0	κ	$u(r_M)$	r_M	$u(r_m)$	r_m	r_{out}	k_1 ($m^3\ s^{-1}$)	k_2 (s^{-1})	k_3 (s^{-1})	τ
4650	200	0.2692	39.5	3.53	205.15	−1.62	219.89	255.23	9.80×10^{-18}	114.18	27.39	0.007
4650	300	0.2785	44.11	12.33	305.48	−1.7	330.37	382.24	9.84×10^{-18}	34	1.76×10^{-3}	0.03
4650	400	0.2825	47.25	23.34	405.85	−1.74	440.89	509.33	9.86×10^{-18}	14.41	1.49×10^{-8}	0.07
4650	600	0.2868	51.53	49.09	606.54	−1.79	661.95	763.64	9.88×10^{-18}	4.28	3.58×10^{-20}	0.23
5800	700	0.2745	44.94	58.66	708.48	−1.68	785.16	910.85	1.02×10^{-17}	2.64	1.59×10^{-24}	0.38
5800	900	0.2763	47.12	86.67	909.22	−1.71	1009.95	1171.05	1.02×10^{-17}	1.24	6.12×10^{-37}	0.81
5800	1000	0.2774	48.03	101.11	1009.56	−1.72	1122.34	1301.16	1.02×10^{-17}	0.91	2.34×10^{-43}	1.1
5800	1200	0.2788	49.59	130.93	1210.21	−1.73	1347.15	1561.38	1.03×10^{-17}	0.52	1.65×10^{-56}	1.91
6000	300	0.2615	36.51	10.78	306.99	−1.57	336.33	391.90	1.02×10^{-17}	33.05	7.30×10^{-3}	0.03
5000	300	0.2729	41.84	11.85	305.87	−1.67	331.90	384.94	9.95×10^{-18}	33.61	2.63×10^{-3}	0.03
4000	300	0.2895	49.84	13.02	304.74	−1.8	326.94	376.79	9.61×10^{-18}	34.2	9.22×10^{-4}	0.03
2500	300	0.3353	74.32	14.82	302.99	−2.15	318.13	361.07	8.97×10^{-18}	34.96	1.78×10^{-4}	0.03
7000	600	0.26	38.06	42.21	609.65	−1.57	682.80	796.04	1.05×10^{-17}	4.11	2.82×10^{-17}	0.24
5000	600	0.2775	48.74	47.99	607.01	−1.74	665.40	769.16	9.99×10^{-18}	4.25	1.05×10^{-19}	0.24
4000	600	0.307	58.08	51.26	605.66	−1.89	655.12	752.50	9.65×10^{-18}	4.32	4.29×10^{-21}	0.23
2500	600	0.3574	106.82	59.3	602.84	−2.44	630.11	706.83	8.65×10^{-18}	4.38	1.65×10^{-24}	0.23

[a] The colloidal systems are all assumed to have a surface potential $\psi_0 = 25$ mV and at temperature 298 K.

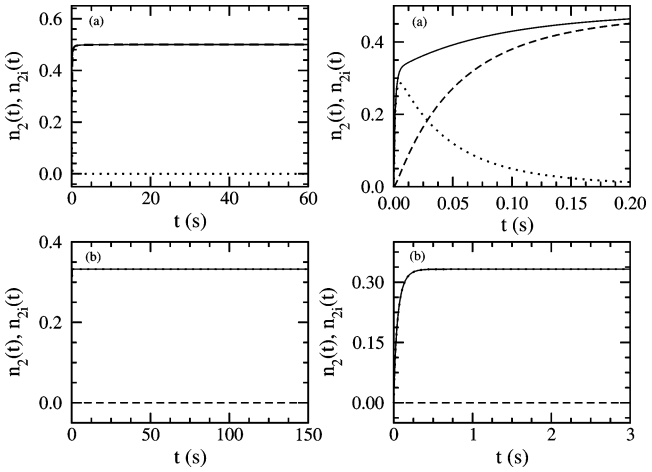

Figure 6. Secondary $n_{2S}(t)$ (dotted curve), primary $n_{2P}(t)$ (dashed curve), and total $n_2(t) = n_{2S}(t) + n_{2P}(t)$ (full curve) concentrations of dimers vs time t (s) calculated for charged colloids (a) fixed at $T_A = 4650$ K with size $\sigma_0 = 200$ nm and (b) fixed at $T_A = 5800$ K with size $\sigma_0 = 700$ nm. The plot on the right-hand side in each row gives the variation of the same quantities but for a very short time.

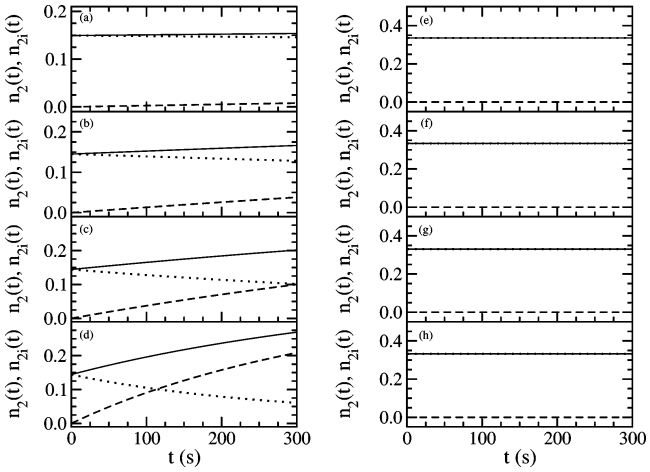

Figure 7. Secondary $n_{2S}(t)$ (dotted curve), primary $n_{2P}(t)$ (dashed curve), and total $n_2(t) = n_{2S}(t) + n_{2P}(t)$ (full curve) concentrations of dimers vs time t (s) calculated for monodisperse charged colloids of size $\sigma_0 = 300$ nm (left column) with T_A at (a) 2500 K, (b) 4000 K, (c) 5000 K, and (d) 6000 K (see Table 3) and of size $\sigma_0 = 600$ nm (right column) with T_A at (e) 2000 K, (f) 4000 K, (g) 5000 K, and (h) 7000 K.

however, the same. Quantitatively, the magnitude of k_2 (k_3) for the systems $T_A = 5800$ K is an order or two smaller (significantly smaller) compared with the systems $T_A = 4650$ K. The second aspect is that the monodisperse systems $\sigma_0 = 300$ nm have their k_2 and k_3 respectively an order and many orders of magnitude larger in comparison with the monodisperse systems $\sigma_0 = 600$ nm. Nevertheless, the trend of change of k_2 (k_3) in these two sets of monodisperse systems is opposite to (the same as) the systems with fixed T_A.

The implication of the first aspect is that the system $T_A = 4650$ K (5800 K) is relatively less (more) stable kinetically. To appreciate this, we scrutinize parts a and b of Figure 6 respectively for ($T_A = 4650$,$\sigma_0 = 200$ nm) and (5800 K,$\sigma_0 = 700$ nm) their temporal variations of $n_{2S}(t)$ and $n_{2P}(t)$. For the former system, it has been predicted previously (see Figure 4 in Lai and Wu[21]) to sustain coexisting stable liquid−liquid with respect to its liquid−solid counterpart. As can be seen from Table 3, $u(r_M)$ is rather low. The present work nevertheless shows that it is unstable kinetically. Figure 6a shows clearly the drastic decrease of $n_{2S}(t)$ to vanishingly small values for $t \geq 0.3$ s after a very short period of increase. In contrast, we see a rapid rise of $n_{2P}(t)$ that after crossing $n_{2S}(t)$ at $t \approx 0.0285$ s increasing monotonically. For the latter system (Figure 6b), the stable liquid−liquid coexistence phases indicate that $n_{2S}(t)$ is predominant whereas $n_{2P}(t)$ is vanishingly small. The reason is that $u(r_M)$ for this suspension is manifestly high ($u(r_M) = 58.66k_BT$). There is, however, a discernible difference in the initial increase of $n_{2S}(t)$ in these two dispersions, namely, it is gradual for $\sigma_0 = 1200$ nm and becomes steeper for $\sigma_0 = 700$ nm.

Coming to the second aspect, the change of k_2 in the direction signaling stable coexisting phases resembles that given in Table 1. The emergence of the stable liquid−liquid coexisting phases is therefore consistent with the kinetic trend. The fact that k_2 for the monodisperse colloids $\sigma_0 = 600$ nm is an order of magnitude smaller and is accompanied by larger $u(r_M)$ generally suggest that these systems are kinetically more stable. To show this, we compare in Figures 7a−d and 7e−h the time development of $n_{2i}(t)$ and $n_2(t)$ for the monodisperse systems $\sigma_0 = 300$ and 600 nm, respectively. For the case $\sigma_0 = 300$ nm, in going from $T_A = 2500$ K (Figure 7a) to $T_A = 6000$ K (Figure

7d), the secondary (primary) dimers $n_{2S}(t)$ ($n_{2P}(t)$) is predicted to decrease (increase) with time t. The increment or decrement is slight at $T_A = 2500$ K but larger at $T_A = 4000$ K. In these latter systems n_{2S} dominates. At $T_A = 5000$ K, the decrement of $n_{2S}(t)$ crosses the increment of $n_{2P}(t)$ at $t \approx 300$ s leading thereafter to the rapid growth of primary dimers. The monodisperse colloids at $T_A = 6000$ K are kinetically less stable for the crossing of n_{2S} and n_{2P} occur at an earlier time $t \approx 113$ s. Note that each of these monodisperse systems has a somewhat lower $u(r_M)$ ($10 \leq u(r_M) \leq 15k_BT$). In contrast, the systems $\sigma_0 = 600$ nm, depicted in parts e−h of Figure 7, generally have higher $u(r_M)$ ($\geq 38k_BT$) and this explains why the n_{2S} is always dominant.

Conclusion

In this work, we study the early stage coagulation kinetics for charged colloidal dispersions using a two-body colloid−colloid potential of mean force theoretically constructed from the statistical mechanical integral equation theory. With the help of this interacting potential and in conjunction with the modified Smoluchoski equation, we calculated the rate constants and used them in the coupled rate equations for dimers to find the number concentrations n_{2i} of secondary (i = S) and primary (i = P) dimers as functions of time. The theory was first applied to an aqueous dispersion of polystyrene latices reported experimentally to display the agglomeration phenomenon. From the change of the rate constants k_i (and hence n_{2i}) with the electrolyte concentration as well as parameters pertinent to colloids, we correlate the trend observed in these quantities to the scenario signaling the transition between the reversible flocculation and the irreversible coagulation. Our theoretical findings for the same kind of transition are compatible with this trend. Then we applied the same methodology to study the coagulation kinetics for aqueous dispersions of charged colloids. On the basis of the energy criterion, these systems were previously predicted to exhibit the stable liquid−liquid coexisting phases. We showed in particular that the colloidal stability derived from the energy criterion consideration does not, as a rule, agree with that predicted by the kinetic criterion. Parenthetically, we remark that the present results of coagulation kinetics are theoretically qualitative since only the dimer formation is assumed. A more rigorous and quantitative analysis of the kinetic criterion should, however, go beyond dimers. A general theory of such kind has been described in the book by Sonntag and Strenge,[31] although the implementation would need a multiparticles potential whose form is at present still unknown for a charged colloidal system.

Acknowledgment. This work is supported in part by the National Science Council under Contact No. NSC92-2112-M-008-033.

LA0476682